Reaction Chemistry & Engineering

ROYAL SOCIETY OF CHEMISTRY

COMMUNICATION

View Article Online
View Journal | View Issue

Cite this: *React. Chem. Eng.*, 2023, **8**, 316

Received 15th September 2022,
Accepted 26th November 2022

DOI: 10.1039/d2re00378c

rsc.li/reaction-engineering

Aminophosphine-based continuous liquid-phase synthesis of InP and InP/ZnS quantum dots in a customized tubular flow reactor†

Zhuang Wang[a] and Doris Segets *[ab]

We present a new platform with a customized flow reactor for the continuous synthesis of InP-based quantum dots (QDs) using greener aminophosphine as phosphorus precursor instead of tris(trimethylsilyl)phosphine. With the benefit of a compact reactor configuration (approx. 30 × 25 × 25 cm^3) and a premixed precursor solution, InP QDs were successfully synthesized with tunable sizes from 2.7 nm to 3.4 nm and narrow particle size distribution (PSD) with relative standard deviation (RSD) down to 7.7%. In addition, as a proof of principle, InP/ZnS core/shell QDs were also successfully synthesized. Without optimization of the synthesis protocol, a photoluminescence quantum yield (PLQY) of 30.9% was achieved.

1. Introduction

Colloidal semiconductor nanocrystals or quantum dots (QDs), as a new class of advanced materials, have been applied in various fields, such as light-emitting devices or solar energy conversion,[1] due to their unique size- and shape-dependent optical and electronic properties. Cd/Pb chalcogenide QDs are the most investigated and developed materials which have been demonstrated to be superior to their counterparts regarding optical properties.[2] However, Cd and Pb are hazardous heavy metals which are restricted in many countries or associations. Therefore, their usage for high performance QD materials is heavily limited. Developing Cd/Pb-free QDs with comparable optical properties is becoming more and more demanding.

Indium phosphide (InP) QDs are typical III–V group semiconductor nanocrystals which feature a large absorption coefficient, broad colour tunability, and low toxicity, which altogether render them promising alternatives to conventional Cd/Pb-based QDs.[3] To date, the synthesis of InP QDs has been facing multiple challenges, one of which is the scarcity of well acclaimed phosphorus precursors (P source). Initially, tris(trimethylsilyl)phosphine (PTMS) was reported as phosphorus precursor[4] and since then it has been the most widely used P source. Ramasamy *et al.* optimized the synthesis protocol yielding InP/ZnS QDs with low emission linewidth of 36 nm and photoluminescence quantum yields (PLQY) up to 67%,[5] which is comparable to those of their Cd-/Pb-based QDs counterparts. However, PTMS is a highly costly and pyrophoric P source which produces PH_3, a highly toxic gas, upon contact with moist air. Consequently, in order to replace PTMS, more economical and relatively greener P source were explored by many researchers, such as P_4,[6] PCl_3[7] and aminophosphines.[8] In particular, aminophosphines have emerged as safer and more economical precursors to produce InP-based QDs with comparable PL properties as those prepared by conventional protocols using PTMS.[9] It has been demonstrated that the aminophosphine-based synthesis and the introduction of ZnS and/or ZnSe shell have resulted in InP/ZnE (E = S, Se) QDs with state-of-the-art emission linewidths down to 46 nm and PLQY up to 60%.[10]

Although aminophosphines provide a cost efficient and environment friendly route to produce heavy metal-free InP-based QDs, their potential scale-up from laboratory batch production remains the key challenge. To date, the majority of reports concerning the aminophosphine-based synthesis of InP-based QDs focused on the typical flask-based hot injection method, which inherently comes with disadvantages when scale-up is considered. Typically mentioned[11,12] were inadequate mixing and heating, poor batch to batch reproducibility which strongly depends on the experience of individuals, limited throughput and segmentation of the production which means when one batch of precursors is consumed the synthesis has to be paused in order to refill

[a] *Chair for Particle Science and Technology, Insitute for Combustion and Gas Dynamics (IVG-PST), University of Duisburg-Essen (UDE), Duisburg, Germany. E-mail: doris.segets@uni-due.de*
[b] *Center for Nanointegration Duisburg-Essen (CENIDE), Duisburg, Germany*

† Electronic supplementary information (ESI) available. See DOI: https://doi.org/10.1039/d2re00378c

precursors. These make it essential to develop continuous processes for the synthesis of InP-based QDs as potential techniques for large-scale production.

The continuous flow synthesis of InP-based QDs was first reported in 2009 by Nightingale and de Mello who synthesized InP QDs using PTMS in a continuous flow microreactor. In their work, the continuous synthesis system consisted of a single channel or double channel injection pump, an oil bath and a flow cell.[13] After this seminal work, Jensen and Bawendi synthesized InP and InP/ZnS core/shell QDs in a continuous multistage microfluidic platform.[14,15] By using their multiple stage platform, a PLQY of as-synthesized InP/ZnS QDs up to 50% was achieved, however FWHM was still relatively large (170–215 nm) and the P source used in their works was still PTMS. In a recent report from their group, aminophosphine as P source was investigated to synthesize InP/ZnS QDs in a newly designed miniature continuous stirred tank reactor (CSTR) cascade.[16] This innovative platform allowed for the continuous synthesis of InP/ZnS QDs exhibiting emission linewidths of 46–64 nm and QY up to 42%. However, with regard to scale up this platform, as adaption of a stirred tank reactor, might still have mixing and heating issues at large scale production. Similarly, Kenis *et al.* also synthesized InP/ZnSe/ZnS QDs using aminophosphine in an automated reconfigurable continuous flow reactor platform where narrow photoluminescence (PL) line widths (~50 nm) and high PLQYs (>50%) were achieved.[17] However, their flow reactor consisted of straight stainless-steel tubes which could be limited by space when the synthesis requires long reaction channels (residence time). In addition, the procedure for the shell formation was quite complicated with multiple injection steps. Reiss *et al.* also investigated the aminophosphine-based synthesis of InP QDs in their continuous flow reactor.[18] However, the as-synthesized InP QDs showed a broad and featureless absorption peak in the UV-vis spectra, indicating a wide PSD.

Herein, we introduce a newly designed high temperature (up to 350 °C) tubular flow synthesis platform with core and shell reactors for the continuous and scalable synthesis of InP and InP/ZnS QDs using a safer and more economical aminophosphine precursor in comparison to standard protocols involving highly pyrophoric and expensive PTMS. Each tubular reactor consists of easily exchangeable and length-wise adjustable stainless-steel tubes. The tubes are wrapped around an aluminum rod with a heating cartridge inserted into the center of the rod which is highly compact regardless of the length of the tube. As no stirred tank reactor is involved, more efficient heating and radial mixing are provided. In addition, a premixed precursor solution was used for the continuous synthesis to reduce complexity from heat and mass transfer to a heat transfer-only development. The synthesized InP core QDs show tunable mean particle sizes from 2.7 nm to 3.4 nm that are achieved by varying temperature and mean residence time in the first core reactor and at the same time exhibit a narrow PSD with a relative standard deviation (RSD) down to 7.7%. Moreover, InP/ZnS core/shell QDs were synthesized by simply introducing an additional S precursor between the core reactor and the shell reactor. The synthesized core/shell QDs showed, without optimization of process parameters, already a high QY of 30.9% and a narrow emission linewidth of 90 nm. Because of its simplicity, compactness and versatility that directly results from the combination of our setup and the use of a premixed precursor solution, our work is dedicated to provide a powerful platform for the scalable production of InP-based QDs using safer and greener aminophosphine precursor chemistry.

2. Experimental

2.1. Chemicals

Indium chloride ($InCl_3$, 99.999%), zinc chloride ($ZnCl_2$, ≥98%), tris(diethylamino)phosphine (PDEA, 97%), and 1-dodecanethiol (DDT, ≥98%) were purchased from Sigma-Aldrich. Oleylamine (80–90%) was purchased from Acros Organics. Ethanol (analytical grade) and *n*-hexane (≥99%) was purchased from VWR Chemicals.

2.2. Flow synthesis of InP and InP/ZnS QDs

Preparation of stock solution: in order to avoid high viscosity, $InCl_3$ and $ZnCl_2$–oleylamine mixture were degassed separately. Briefly, 884.72 mg (4 mmol) of $InCl_3$ was added into a three-neck flask containing 20 mL of oleylamine. The mixture was stirred and degassed at 120 °C for 1 h. Similarly, 2.7257 g (20 mmol) of $ZnCl_2$ was added into a three-neck flask containing 20 mL oleylamine and the mixture was stirred and degassed at 120 °C for 1 h. Then the above solutions were mixed and stirred vigorously inside a glovebox (N_2 atmosphere, $O_2 < 20$ ppm, $H_2O < 20$ ppm) for 2 h. 4.4 mL (16 mmol) of tris(diethylamino)phosphine (PDEA) was added into the above mixture of $InCl_3$, $ZnCl_2$ and oleylamine and stirred in the glovebox for further 6 h in order to fully mix the precursors. During stirring, gas bubbles were observed. After 6 h of mixing, a colorless and transparent precursor solution was obtained and used as stock solution for the flow synthesis of InP-based QDs.

Flow synthesis of InP QDs and InP/ZnS QDs: all syntheses were performed in a glovebox and are based on a modified synthetic protocol of Kenis *et al.*[17] The modifications were that a premixed stock solution was utilized instead of the inline mixing and that 1-dodecanethiol (DDT) was used as the sulfur source instead of trioctylphosphine-S (TOP-S). For the InP core synthesis, the above prepared stock solution was aspirated into the syringe and the reaction solution was pumped through the heating box (flow rate ranging from 0.05–0.3 mL min^{-1} which results in mean residence times from 12 min to 72 min) at high temperature (variations from 180–250 °C). As-synthesized InP QDs then were collected (2–5 mL) at the outlet of the reaction channel, flocculated by the addition of ethanol ($V_{crude\ solution}:V_{ethanol} = 1:3$ at room temperature) and washed by centrifugation at 10 000 rpm for

10 min ($V_{n\text{-hexane}}:V_{\text{ethanol}}$ = 1 : 5). The washing step was repeated three times and finally the obtained pellet containing InP QDs was redispersed in *n*-hexane for further analysis. For the synthesis of InP/ZnS core–shell QDs, instead of collecting the InP QDs, the reaction solution continued flowing and was mixed with 1-dodecanethiol (DDT). The above mixture was then fed into the second heating box (*T*: 200 °C, InP core QDs flow: 0.06 mL min^{-1}, DDT flow: 0.03 mL min^{-1}). The as-synthesized InP/ZnS core/shell QDs were collected at the outlet, washed by centrifugation and redispersed in *n*-hexane for further analysis.

2.3. Characterization

All UV-vis absorption measurements were conducted using an ultra-low stray light fiber optic UV-vis-NIR spectrometer with replaceable slit, 2048 pixel/14 × 200 μm CMOS detector and deuterium–halogen light source offering a wavelength range from 400 to 900 nm. For all measurements, the optical path length was 1 mm. X-ray diffraction (XRD) patterns were collected in a high-resolution powder X-ray diffractometer (Cu anode, 0.154 nm, Malvern Panalytical X'Pert MPD PW3040). The sample was prepared by drop-casting the QD dispersion on a silicon wafer. Transmission Electron Microscopy (TEM) images were acquired using a JEOL JEM 2200FS. For TEM sample preparation, the diluted QD dispersion was drop-casted on a carbon coated copper TEM grid and stored inside a nitrogen-filled glovebox for drying. PL spectra were recorded at room temperature by a HORIBA JOBIN YVON Fluorolog®-3 spectrofluorometer under 400 nm excitation. The PLQY for the InP/ZnS QDs was determined by the integrating sphere accessory F-3018 which recorded the excitation-source intensity and calculated the area under the corrected emission spectra.

2.4. Particle size distribution (PSD) from UV-vis absorption spectra

PSDs of InP QDs in this work were extracted from UV-vis spectra according to our previous report on PSD determination of CdSe QDs[12] from deconvolution of UV-vis absorption spectra. The framework for the derivation of a PSD (resulting in the equivalent sphere of the semiconducting volume) from optical absorbance spectra was originally published by Segets *et al.*[19,20] Here, an InP bulk band gap of 1.35 eV was used and the size-dependent band gap energy was acquired based on data of Cho *et al.*,[21] Baskoutas *et al.*,[22] Fu *et al.*,[23] Ferreyra *et al.*,[24] Guzelian *et al.*,[25] Yu *et al.*,[26] Goyal *et al.*[27] and Li *et al.*[28]

The balanced mean particle size by volume ($x_{1,3}$) was calculated from the volume density distribution (q_3) derived from UV-vis absorption spectra:

$$x_{1,3} = \int_{\text{xmin}}^{\text{xmax}} x q_3(x)\mathrm{d}x \quad (1)$$

The standard deviation (σ) was calculated as:

$$\sigma = \sqrt{\int_{\text{xmin}}^{\text{xmax}} (x - x_{1,3})^2 q_3(x)\mathrm{d}x} \quad (2)$$

Finally, $x_{1,3}$ and σ were combined to derive the dimensionless relative standard deviation (RSD):

$$\text{RSD} = \frac{\sigma}{x_{1,3}} \quad (3)$$

3. Results and discussion

Fig. 1 shows the continuous flow synthesis platform with the customized tubular flow reactor placed in a glovebox. The key components are the precursor reservoir, the syringe pump system, and two heating boxes. The precursor reservoir contains the reaction stock solution which can be prepared as described in the experimental section. The syringe pump system was manufactured by ayxesis GmbH and consists of a power supply module, a movement controller module, a syringe (2.5 mL, 20 bar) and controlling software (SyPuControl V1.2.2.0). Noteworthy, the whole setup can be operated with two alternating syringes in parallel to achieve a truly continuous flow. The two heating boxes HB1 and HB2 were manufactured by IMPCO-Metall GmbH and are mainly made of stainless-steel. Both boxes have three identical heating units. Each of them includes a stainless-steel spiral (outer diameter OD = 1/16″, inner diameter ID = 0.9975 mm, stretched length approx. 4.6 m) which enables mean residence times from 2.4 min at a flow rate of 1.5 mL min^{-1} to 120 min at a flow rate of 0.03 mL min^{-1} and an aluminum block equipped with three high-performance heating cartridges. HB1 can hold temperatures up to 350 °C (for nucleation/growth) and HB2 up to 220 °C (for shell formation) respectively.

Before starting the flow synthesis, as described in the following, the strategy of mixing two precursors is highly important. In a continuous synthesis platform, there are generally two options for good mixing:

a) Using a T-mixer inherently requires the generation of a high-pressure loss and thus high flow rates to dissipate energy by turbulence for good meso- and micromixing.[29–32] However, this comes with the drawback that higher flow rates require noticeable amounts of stock solution and thus result in a high precursor consumption per unit time. At the same time, in case of a certain residence time to be kept constant for a required reaction progress, higher flow rates require longer tube lengths. Long tubes are usually not recommended in terms of space saving and handling (*e.g.*, back-diffusion, axial dispersion, residence time distribution). Thus, the use of T-mixers comes to limitations when syntheses require fast mixing and long residence times.

b) Using low flow rates, sophisticated split and recombined mixers for good mixing.[14,17] This however requires complicated, costly equipment which is often easily clogged.

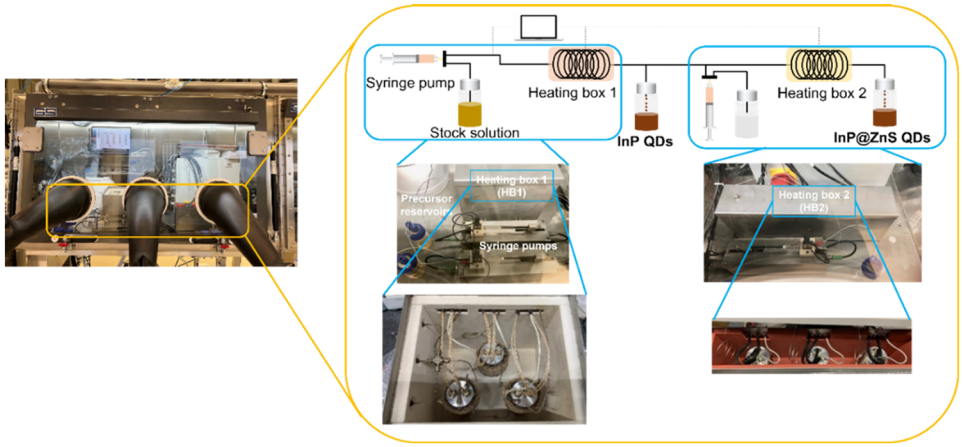

Fig. 1 Schematic of the continuous flow synthesis platform for the synthesis of InP core and InP/ZnS core–shell QDs consisting of pumps for dosing at constant pressure (core and shell) and two heating boxes (heating box HB1 for the InP core, heating box HB2 for the ZnS shell).

None of these options matched our intention in the context of the synthesis of InP/ZnS QDs. Inspired by works on $CuInS_2$ QDs,[33,34] we came up with the idea to transfer the hot injection process to a simple heating up synthesis which is to start from a premixed solution of all precursors before the synthesis is initiated by high temperature in the reactor. This reduces the complexity of particle formation from a heat and mass transfer problem to a heat transfer-only problem.

As described above, a simple premixed precursor solution was prepared where the [In] and [P] precursors were mixed thoroughly beforehand. Our aim was to overcome the issue related to inadequate mixing which causes broad PSD and thus leads to poor optical properties.[12] Fig. 2a shows a typical XRD pattern of the as-synthesized InP QDs. The corresponding peak positions for the synthesized InP QDs are in good agreement with zinc blende structured InP bulk data. In line with the expectations, due to a significant reduction in crystal size, a remarkable peak broadening was observed. From the TEM image in Fig. 2b and Fig. S1,† it can be carefully concluded that the InP QDs synthesized at 180 °C and 0.1 mL min^{-1} exhibit a rather irregular, quasi-tetrahedral shape. This observation agrees well with the previous reports.[35–37] The low image quality originates from organic ligands attached to the InP QD surface, which however, does not affect the conclusion drawn in this work. With regard to their optical properties, it can be seen that the absorption peak at 518 nm in the UV-vis absorption spectrum of the synthesized InP QDs was observed which is the characteristic first excitonic absorption peak of InP (Fig. 2c). Moreover, the PSD was derived from the UV-vis spectrum as shown in the inset graph of Fig. 2c which matches well with the PSD obtained from TEM image analysis. The balanced mean particle size by volume derived from the UV-vis spectrum was 2.7 nm. The above results demonstrate the successful synthesis of InP QDs using our newly designed continuous flow synthesis platform with a tubular flow reactor. Moreover, InP QDs synthesized at 180 °C and 200 °C from different syntheses using our platform show good reproducibility in terms of UV-vis absorption spectra (#1 and #2 were synthesized using the same stock solution at different days; #2 and #3 were synthesized using different stock solution).

Because of the quantum confinement effect, the optical properties are strongly dependent on the size of QDs.

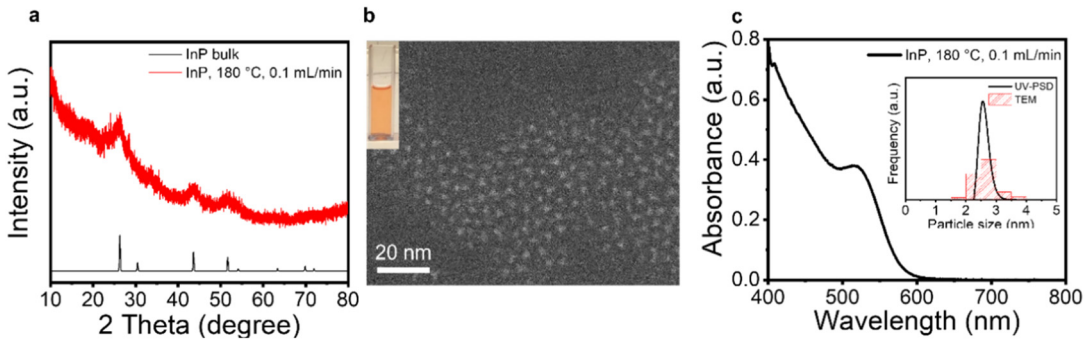

Fig. 2 (a) XRD measurement, (b) TEM image and (c) UV-vis absorption spectrum of InP QDs synthesized at 180 °C and 0.1 mL min^{-1}. The inset in (b) shows the InP QD dispersion obtained after washing and the inset in (c) shows the direct comparison of the PSD derived from the UV-vis data and the PSD derived from TEM (101 particles were analysed and evaluated by ImageJ).

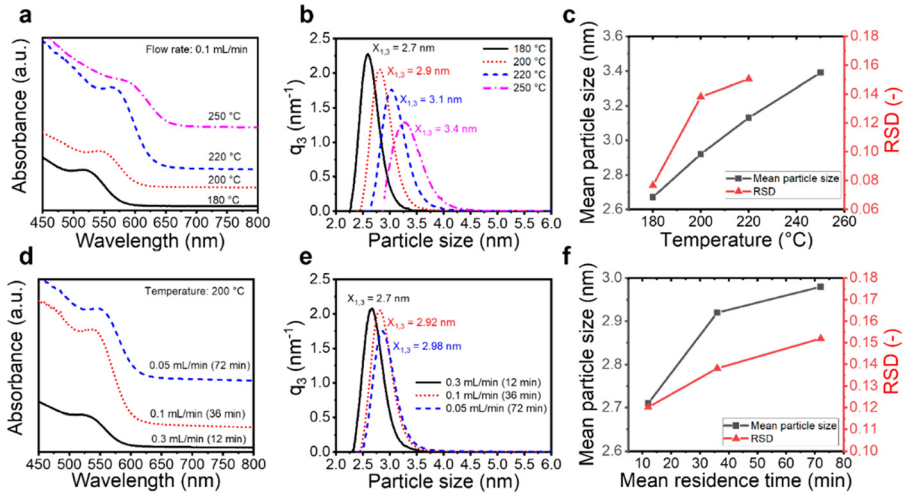

Fig. 3 (a and d) UV-vis absorption spectra, (b and e) corresponding PSDs and (c and f) mean particle size and RSD of InP QDs synthesized at different temperatures and flow rates. Experimental conditions: a–c at 0.1 mL min^{-1} and 180–250 °C; d–f at 200 °C and 0.05–0.3 mL min^{-1}.

Therefore, size tunability is highly important. In order to analyse this, in a first series of experiments, we varied temperature and residence time during InP QD formation to tune the particle size. It can be seen that with increasing the core reaction temperature from 180 °C to 250 °C, the absorption peak shifts from 518 nm to 590 nm (Fig. 3a). The PSDs derived from the spectra showed mean particle sizes from 2.7 nm to 3.4 nm respectively (Fig. 3b). The resulting RSD, indicating dispersity, was also calculated (Fig. 3c). It showed that with the increase of reaction temperature, the PSD broadened. This is in line with findings of Buffard *et al.*, and can be ascribed to a rapid nucleation burst at high temperature that is however followed by partial dissolution of small QDs which might be associated with ripening.[35] When comparing the influence of reaction temperature (upper row, Fig. 3a–c) and residence time (lower row, Fig. 3d–f), the particle size seems less sensitive to changes of the latter. As can be seen in Fig. 3d and e, the absorption peak only shifted from 529 nm to 549 nm when the flow rate was varied from 0.05 mL min^{-1} to 0.3 mL min^{-1}, corresponding to mean particle sizes from 2.7 nm to 3.0 nm. Similarly, also with increasing the residence time, the PSD broadened which might also be related to the onset of ripening (Fig. 3f). In addition, in order to evaluate the production ability with the investigated process parameters, the chemical yield and estimated production rate have been calculated according to Hens, *et al.*[10] and are shown in Tables S1 and S2.† The highest production rate of our platform for synthesizing InP QDs is 107 mg h^{-1} with a conversion of 73.6%.

After demonstrating the successful generation of InP core particles, direct shelling was applied. It is believed that direct shelling in one synthesis run is desired to prevent chemical deterioration of the core surface and enhance the PL properties. As a proof of principle for direct shell formation, the synthesis of core/shell QDs using our tubular flow synthesis platform was implemented. The second heating box (HB2) for shell formation was installed after the core heating box (HB1). Between the core and the shell heating box, a suitable sulfur precursor (DDT) was injected. The core synthesis was conducted at 200 °C and 0.06 mL min^{-1} and the shell formation was performed at 200 °C and 0.03 mL min^{-1} (DDT stream). The UV-vis and PL spectra are presented in Fig. 4a. The first excitonic absorption peak at 530 nm and the emission peak at 607 nm for the synthesized InP/ZnS QDs are clearly observed. The observed asymmetry in the PL spectrum might result from surface defects.[38] Under UV irradiation, the synthesized InP/ZnS core/shell QDs are luminescent and emit yellowish colour under 365 nm excitation (Fig. 4b). Further the PLQY was measured to be 30.9% which is comparable to that of InP-based core/shell QDs in recent publications using similar synthesis

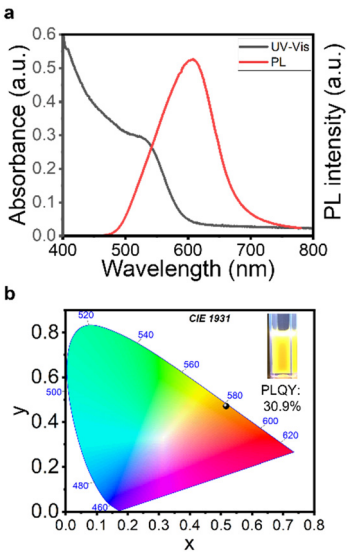

Fig. 4 (a) UV-vis absorption, PL spectrum and (b) CIE 1931 color space chromaticity diagram of InP/ZnS QDs synthesized in our continuous flow setup. The inset in (b) shows the photograph of the corresponding InP/ZnS QDs colloid solution under 356 nm UV irradiation and PLQY.

protocols.[16,17] Although the PL properties need to be further tuned to realize QD emissions that enable to cover the whole visible range and PLQY needs to be improved by shelling optimization (process optimization,[39] double shell structure,[17,40] *etc.*), our results clearly evidence the high potential of our continuous flow synthesis setup. With >30% PLQY, the generated InP/ZnS QDs exhibit excellent optical properties that can be achieved by an easy, comparatively green and scalable process using a very compact and easy to handle flow platform.

4. Conclusion

In summary, we demonstrated the successful application of a continuous synthesis platform with a customized tubular flow reactor and a premixed precursor solution for facile synthesis of InP QDs and InP/ZnS core/shell QDs using aminophosphine-based reaction chemistry. A premixed precursor solution was evidenced as an effective strategy for achieving narrow PSDs. The particle size of the synthesized InP QDs could be tuned from 2.7 nm to 3.4 nm (balanced mean particle size by volume) by simply varying temperature and residence time and exhibited relative standard deviations (RSD) from 7.7 to 17.5%. InP/ZnS core/shell QDs were achieved by simply introducing an additional sulfur containing precursor between the core and the shell reactor. The synthesized core/shell QDs – without process optimization – showed a comparably high QY of 30.9% and a narrow emission linewidth of 90 nm. In order to further improve the PLQY of InP/ZnS core/shell QDs using the herein described continuous and greener route, further investigations will focus in threefold direction. First, for improvement of the size uniformity of the core QDs generated by the developed continuous flow synthesis setup, we will systematically optimize the precursor concentration, the In/Zn mole ratio and the flow profile. Second, the shell formation will be analyzed in detail, including the shell composition, the shell thickness, and the incorporation of an inner shell made from ZnSe. Finally, the continuous flow synthesis platform itself will be advanced further by integration of inline UV-vis and PL analytics for real time screening of reaction parameters and assessment of particle formation kinetics in combination with flow tubes of varying length and process control. Our work is dedicated to provide a versatile synthesis platform for the continuous production of InP based QDs using safer and greener aminophosphine precursor and pave the way for the industrial application of III–V core/shell QDs in optoelectronics.

Conflicts of interest

There are no conflicts to declare.

Acknowledgements

The authors thank Ludger Jerig and Dr. Sebastian Hardt for their help in manufacturing the continuous setup and thank ICAN and Paolo Fortugno at University of Duisburg-Essen for their support in quantum dots characterization. We are also thankful for the funding of the Collaborative Research Centre 1411 "Design of Particulate Products" (Project-ID 416229255) provided by Deutsche Forschungsgemeinschaft (DFG, German Research Foundation).

Notes and references

1 F. P. Garcia de Arquer, D. V. Talapin, V. I. Klimov, Y. Arakawa, M. Bayer and E. H. Sargent, *Science*, 2021, **373**, 640.
2 C. B. Murray, D. J. Norris and M. G. Bawendi, *J. Am. Chem. Soc.*, 1993, **115**, 8706–8715.
3 B. Chen, D. Y. Li and F. Wang, *Small*, 2020, **16**, 2002454.
4 O. I. Micic, C. J. Curtis, K. M. Jones, J. R. Sprague and A. J. Nozik, *J. Phys. Chem.*, 1994, **98**, 4966–4969.
5 P. Ramasamy, N. Kim, Y. S. Kang, O. Ramirez and J. S. Lee, *Chem. Mater.*, 2017, **29**, 6893–6899.
6 E. Bang, Y. Choi, J. Cho, Y. H. Suh, H. W. Ban, J. S. Son and J. Park, *Chem. Mater.*, 2017, **29**, 4236–4243.
7 Z. P. Liu, A. Kumbhar, D. Xu, J. Zhang, Z. Y. Sun and J. Y. Fang, *Angew. Chem., Int. Ed.*, 2008, **47**, 3540–3542.
8 W. S. Song, H. S. Lee, J. C. Lee, D. S. Jang, Y. Choi, M. Choi and H. Yang, *J. Nanopart. Res.*, 2013, **15**, 1750.
9 Y. H. Won, O. Cho, T. Kim, D. Y. Chung, T. Kim, H. Chung, H. Jang, J. Lee, D. Kim and E. Jang, *Nature*, 2019, **575**, 634–638.
10 M. D. Tessier, D. Dupont, K. De Nolf, J. De Roo and Z. Hens, *Chem. Mater.*, 2015, **27**, 4893–4898.
11 S. Kubendhiran, Z. Bao, K. Dave and R. S. Liu, *ACS Appl. Nano Mater.*, 2019, **2**, 1773–1790.
12 A. M. Salaheldin, J. Walter, P. Herre, I. Levchuk, Y. Jabbari, J. M. Kolle, C. J. Brabec, W. Peukert and D. Segets, *Chem. Eng. J.*, 2017, **320**, 232–243.
13 A. M. Nightingale and J. C. de Mello, *ChemPhysChem*, 2009, **10**, 2612–2614.
14 J. Baek, P. M. Allen, M. G. Bawendi and K. F. Jensen, *Angew. Chem., Int. Ed.*, 2011, **50**, 627–630.
15 J. Baek, Y. Shen, I. Lignos, M. G. Bawendi and K. F. Jensen, *Angew. Chem., Int. Ed.*, 2018, **57**, 10915–10918.
16 I. Lignos, Y. Mo, L. Carayannopoulos, M. Ginterseder, M. G. Bawendi and K. F. Jensen, *React. Chem. Eng.*, 2021, **6**, 459–464.
17 A. Vikram, A. Zahid, S. S. Bhargava, H. Jang, A. Sutrisno, A. Khare, P. Trefonas, M. Shim and P. J. A. Kenis, *ACS Appl. Nano Mater.*, 2020, **3**, 12325–12333.
18 T. Akdas and P. Reiss, *J. Phys.: Conf. Ser.*, 2019, **1323**, 012007.
19 D. Segets, J. Gradl, R. K. Taylor, V. Vassilev and W. Peukert, *ACS Nano*, 2009, **3**, 1703–1710.
20 D. Segets, J. M. Lucas, R. N. K. Taylor, M. Scheele, H. M. Zheng, A. P. Alivisatos and W. Peukert, *ACS Nano*, 2012, **6**, 9021–9032.
21 E. Cho, H. Jang, J. Lee and E. Jang, *Nanotechnology*, 2013, **24**, 215201.
22 S. Baskoutas and A. F. Terzis, *J. Appl. Phys.*, 2006, **99**, 013708.

23 H. X. Fu and A. Zunger, *Phys. Rev. B: Condens. Matter Mater. Phys.*, 1997, **56**, 1496–1508.
24 J. M. Ferreyra and C. R. Proetto, *Phys. Rev. B: Condens. Matter Mater. Phys.*, 1999, **60**, 10672–10675.
25 A. A. Guzelian, J. E. B. Katari, A. V. Kadavanich, U. Banin, K. Hamad, E. Juban, A. P. Alivisatos, R. H. Wolters, C. C. Arnold and J. R. Heath, *J. Phys. Chem.*, 1996, **100**, 7212–7219.
26 H. Yu, J. B. Li, R. A. Loomis, L. W. Wang and W. E. Buhro, *Nat. Mater.*, 2003, **2**, 517–520.
27 M. Goyal and M. Singh, *Appl. Phys. A: Mater. Sci. Process.*, 2020, **126**, 176.
28 M. Li and J. C. Li, *Mater. Lett.*, 2006, **60**, 2526–2529.
29 J. Gradl, H. C. Schwarzer, F. Schwertfirm, M. Manhart and W. Peukert, *Chem. Eng. Process.*, 2006, **45**, 908–916.
30 L. Metzger and M. Kind, *Chem. Eng. Sci.*, 2017, **169**, 284–298.
31 J. R. Bourne and G. Tovstiga, *Chem. Eng. Res. Des.*, 1988, **66**, 26–32.
32 J. Badyga and R. Pohorecki, *Chem. Eng. J. Biochem. Eng. J.*, 1995, **58**, 183–195.
33 H. Azimi, T. Heumuller, A. Gerl, G. Matt, P. Kubis, M. Distaso, R. Ahmad, T. Akdas, M. Richter, W. Peukert and C. J. Brabec, *Adv. Energy Mater.*, 2013, **3**, 1589–1596.
34 T. Akdas, M. Distaso, S. Kuhri, B. Winter, B. Birajdar, E. Spiecker, D. M. Guldi and W. Peukert, *J. Colloid Interface Sci.*, 2015, **445**, 337–347.
35 A. Buffard, S. Dreyfuss, B. Nadal, H. Heuclin, X. Xu, G. Patriarche, N. Mézailles and B. Dubertret, *Chem. Mater.*, 2016, **28**, 5925–5934.
36 B. M. McMurtry, K. Qan, J. K. Teglasi, A. K. Swarnakar, J. De Roo and J. S. Owen, *Chem. Mater.*, 2020, **32**, 4358–4368.
37 Y. Kim, H. Choi, Y. Lee, W. K. Koh, E. Cho, T. Kim, H. Kim, Y. H. Kim, H. Y. Jeong and S. Jeong, *Nat. Commun.*, 2021, **12**, 4454.
38 E. Cho, T. Kim, S. M. Choi, H. Jang, K. Ming and E. Jang, *ACS Appl. Nano Mater.*, 2018, **1**, 7106–7114.
39 K. Kim, S. Jeong, J. Y. Woo and C. S. Han, *Nanotechnology*, 2012, **23**, 065602.
40 P. Liu, Y. J. Lou, S. H. Ding, W. D. Zhang, Z. H. Wu, H. C. Yang, B. Xu, K. Wang and X. W. Sun, *Adv. Funct. Mater.*, 2021, **31**, 2008453.